



Analysis of land subsidence changes on the Beijing Plain from 2004 to 2015

Lin Guo^{1,2}, Huili Gong^{1,2}, Xiaojuan Li^{1,2}, Lin Zhu^{1,2}, Wei Lv³, and Mingyuan Lyu^{1,2}

¹College of Resource Environment and Tourism, Capital Normal University, Beijing 100048, China

²Beijing Laboratory of Water Resources Security, Capital Normal University, Beijing 100048, China

³Chinese Academy of Calligraphy Culture, Capital Normal University, Beijing 100048, China

Correspondence: Huili Gong (4039@cnu.edu.cn) and Lin Zhu (hi-zhulin@163.com)

Published: 22 April 2020

Abstract. Land subsidence, as a surface response to the development, utilization and evolution of underground space, has become a global and multidisciplinary complex geological environment problem. Since the 1960s, land subsidence has been developing rapidly in the Beijing Plain area. Against the backdrop of the integration of Beijing, Tianjin and Hebei in addition to “southern water” (South-to-North Water Diversion Project, SNWDP) entering Beijing, the systematic study of the evolution mechanism of land subsidence is of great significance for the sustainable development of the regional economy. Firstly, this study used ENVISAT ASAR and RADARSAT-2 data to obtain surface deformation information for the Beijing Plain area from 2004 to 2015 and then verified the results. Secondly, the study area was divided into units using a 960 m × 960 m grid, and the ground settlement rate of each grid unit from 2004 to 2015 was obtained. Finally, the Mann–Kendall test was performed on the grid to obtain the mutation information for each grid unit. Combined with hydrogeology and basic geological conditions, we have attempted to analyze the causes of the mutations in the grid. The results show that 2347 grid cells were mutated in a single year, with most of these distributed across the Yongding River alluvial fan and the middle and lower parts of the Chaobai River alluvial fan. A total of 1128 grid cells were mutated in multiple years, with the majority of these cells mainly distributed across the upper-middle area of the alluvial fan, near the emergency water source and at the edge of the groundwater funnel. This study aims to provide favorable technical support and a scientific basis for urban construction in Beijing.

1 Introduction

At present, more than 150 countries and regions have suffered land subsidence, which has caused huge security risks and economic losses (Gong et al., 2018). Land subsidence in China mainly occurs in the North China Plain (Gao et al., 2018), the Yangtze River Delta (Yin et al., 2016), the Fenwei Basin (Xue et al., 2005) and the Pearl River Delta (Ye et al., 2015), and it presents significant regional differences. Among these differences, the continuous land subsidence in the North China Plain continues to increase (Zhang et al., 2016), the Yangtze River Delta region’s subsidence has been effectively controlled and the Fenwei Basin region’s subsidence is still developing rapidly.

From the perspective of land subsidence monitoring technology, interferometric synthetic aperture radar (InSAR) has become a new ground observation technique over the past 20 years (Ferretti et al., 2000). Compared with traditional technology, InSAR has the advantages of a wide monitoring range and high monitoring accuracy and has been widely used in ground subsidence monitoring research by experts and scholars (Castellazzi et al., 2016; Albano et al., 2016; Amighpey et al., 2016; Dehghani et al., 2013; Ge et al., 2014; Da Lio and Tosi, 2018?). In 2002 and 2004, Berardino and Lanari et al. proposed the small baseline set interferometry–interferometric synthetic aperture radar (SBAS-InSAR) technique, which is more suitable for long time, slow deformation surface monitoring (Berardino et al., 2002; Lanari et al., 2004). Subsequently, experts and schol-

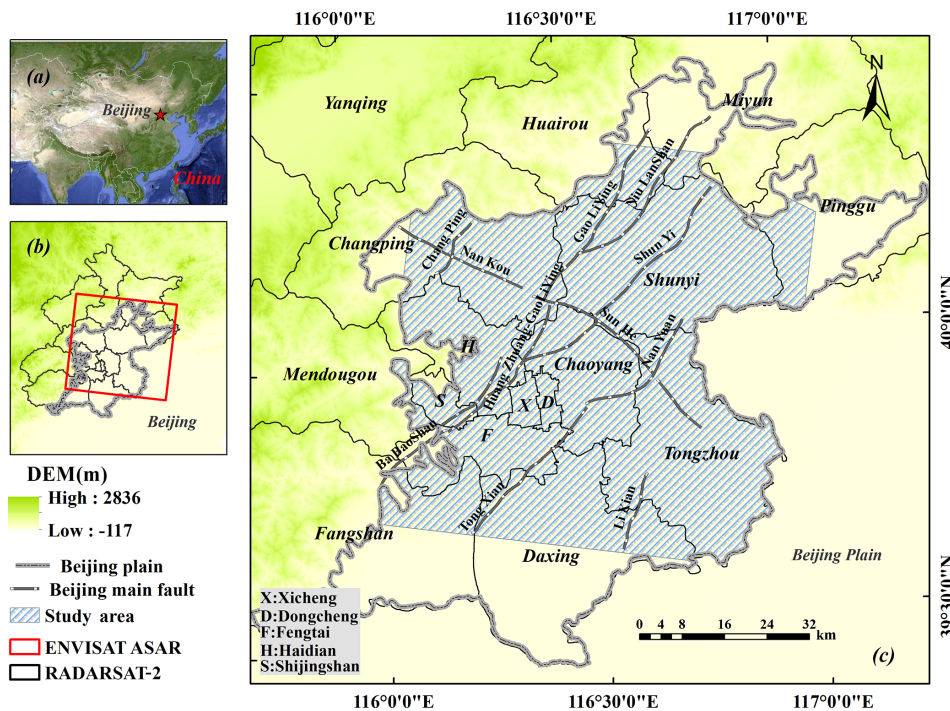


Figure 1. Geographical location of the study area.

ars have used this technology to select multisource SAR data, such as ENVISAT ASAR and COSMO-SkyMed, and have used these data to monitor the surface deformation of the Gulf of Naples (Solari et al., 2018), Los Angeles (Chilingar and Endres, 2005), Central Mexico and other areas (Castellazzi et al., 2016). From the perspective of the evolution mechanism of ground subsidence, the causes of the occurrence and evolution of ground subsidence include both natural and anthropogenic factors. For a long time, experts and scholars have focused more on ground subsidence caused by human factors, including groundwater exploitation, mining, dynamic load and so on (Zhu et al., 2015). Against the backdrop of strong manual intervention in regional water circulation, the identification of land subsidence changes in Beijing can provide technical support for the rational allocation of water resources.

2 Materials and methods

2.1 Study area

Beijing, as the capital of China, is the center of national politics, economy and culture and is an international metropolis with a population of nearly 20 million people (Zhou et al., 2017). In general, the surface elevation in Beijing is between 8 and 2303 m, and it is higher in the northwest and lower in the southeast (Zhou et al., 2017) (Fig. 1). The locations and the hydrogeological conditions of the study region are described in detail in a previous study (Guo et al.,

2019). The ground subsidence in Beijing began in 1935, and the main subsidence regions were located in Xidan and Dongdan. Since the 1970s, land subsidence rates on the Beijing Plain have significantly increased due to the pumping of underground water. In general, the subsidence area is divided into two major areas – “North” and “South” – as well as seven subsidence centers. The North area is located in the east and north of Beijing and includes the Chaoyang, Tongzhou, Changping, Haidian and Shunyi districts. Among them, the Chaoyang and Tongzhou subsidence areas in the east of the plain are contiguous and are Beijing’s fastest (with respect to change) and largest subsidence regions. The subsidence rates of the four subsidence centers in the urban areas of Chaoyang (Jinzhan, Heizhuanghu and Sanjianfang) and Tongzhou have exceeded 100 mm yr^{-1} for many years. The subsidence center in the north of the plain comprises the Changping Baxianzhuang and Haidian Xi Xiaoying areas. In the South area, which is mainly located in Daxing, the primary subsidence center is Lixian. On the whole, the land subsidence rates in the east of the plain are highest, followed by the northern region. Subsidence in the South area mainly occurs in the vicinity of Hebei.

2.2 Processing of SBAS-InSAR and PS-InSAR data from the Beijing Plain from 2004 to 2015

This study used 47 ENVISAT ASAR data from June 2003 to October 2010 and 48 RADARSAT-2 data from November 2010 to December 2015. The Doris-StaMPS algorithm

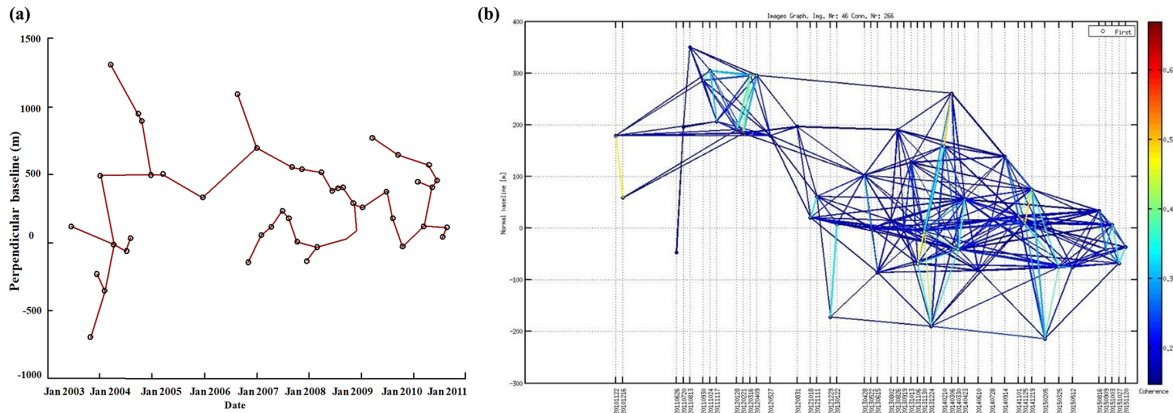


Figure 2. Panel (a) shows the small baseline segment from 2003 to 2010 obtained using SBAS-InSAR. Panel (b) shows the small baseline set from 2010 to 2015 obtained using Quisin-PSInSAR.

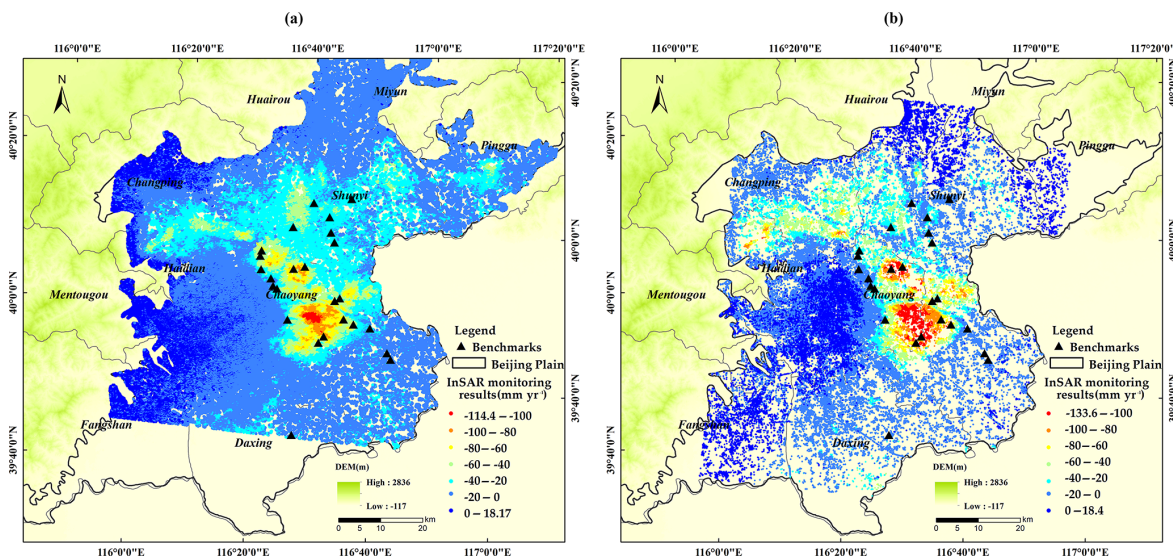


Figure 3. The average land subsidence rate map of the Beijing Plain from 2004 to 2015. Panel (a) is the average rate from 2004 to 2010, and panel (b) is the average rate from 2010 to 2015.

and commercial SARPROZ software were used to analyze the SAR data. The small baseline segments are shown in Fig. 2.

3 Results and discussion

3.1 Acquisition of the land displacement information for the Beijing Plain from 2004 to 2015

Based on the surface deformation monitored by SBAS-InSAR and Quisin-PSInSAR, and using the ArcGIS spatial analysis platform, the displacement rate map of the Beijing Plain area was obtained (Fig. 3). From 2004 to 2010, the average deformation rate ranged from -114.4 to $+18.17$ mm yr^{-1} . The area where the subsidence rate exceeded 25 mm yr^{-1} reached 1078.5 km^2 , which accounted

for 17.2% of the total area of the Beijing Plain. From 2011 to 2015, the average deformation rate ranged from -133.57 to 18.44 mm yr^{-1} .

3.2 InSAR validation

The benchmarks from 2003 to 2013 were selected for validation (Fig. 4). The benchmarks were taken as the original point, and all of the monitoring points within a radius of 150 m were extracted. As can be seen from Fig. 4, the correlation coefficient for the InSAR monitoring results and the level monitoring results from 2003 to 2010 is 0.95 . From 2011 to 2013, the correlation coefficient for the InSAR monitoring results and the level monitoring results is 0.99 .

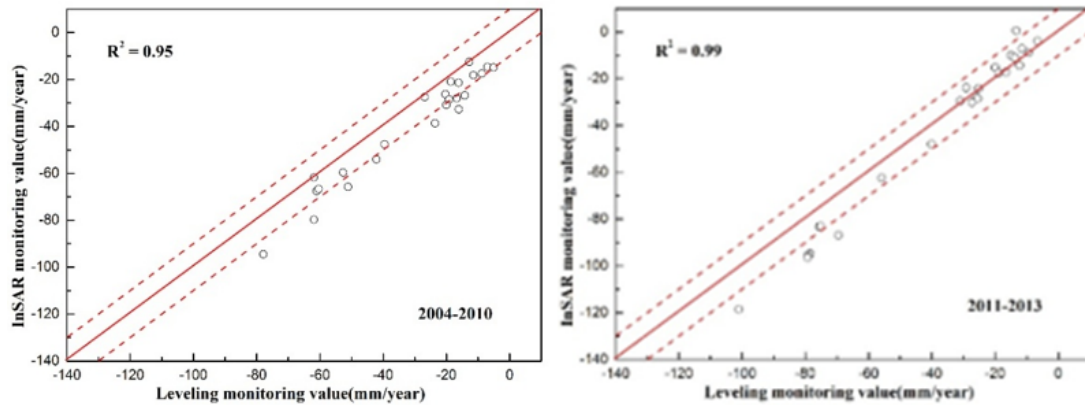


Figure 4. The validation map between InSAR and benchmarks from 2003 to 2013.

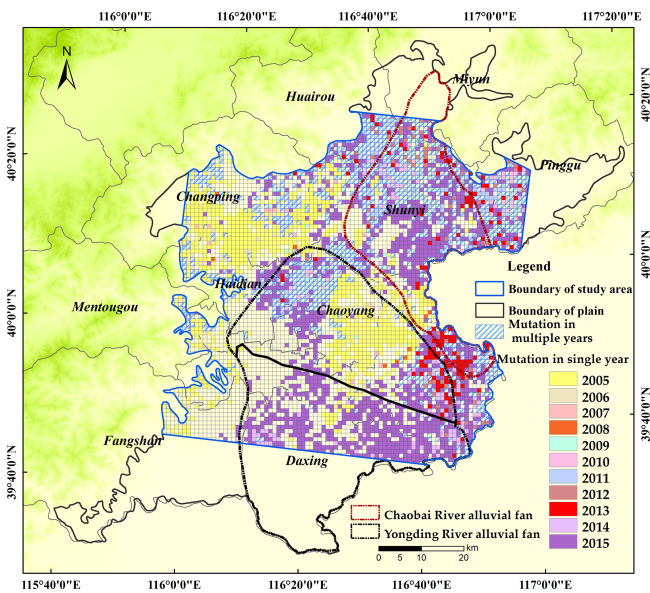


Figure 5. Land subsidence changes (land subsidence rate) results for the Beijing Plain from 2004 to 2015.

3.3 The Mann–Kendall test for land subsidence on the Beijing Plain

In this research, the Mann–Kendall test was used to detect the trend change in land subsidence on the Beijing Plain. Firstly, the research area was divided into a 960 m×960 m grid using the Create Fishnet tool in ArcGIS. Secondly, according to the information from the persistent scatterer (PS) points from 2004 to 2015 that were acquired using InSAR technology, the displacement information from each grid was obtained by utilizing the Spatial Join function in ArcGIS. Finally, the Mann–Kendall test was performed on each grid using Python, and the changes in land subsidence on the Beijing Plain were obtained (Fig. 5).

3.4 Discussion

Figure 5 shows that the grid with single-year mutation is mostly distributed in the middle and the lower part of the Chaobai River alluvial–diluvial fan and the Yongding River alluvial–diluvial fan, and that the grid with multiple-year mutations is mostly distributed at the top of the alluvial–diluvial fan. The reason for this may be that the main factor causing land subsidence on the Beijing Plain is drastic drops in the groundwater level of the Quaternary system, which result in a decrease in the pore water pressure in the overburden layer and a loss of water in the soil layer due to the pumping of underground water. However, in the middle and upper part of the alluvial fan, the deposits have a good permeability, and the groundwater level fluctuates greatly due to the influence of precipitation. The rainfall in different years and the rainfall intensity during the flood season have some different characteristics that may cause the groundwater level in the middle and upper part of the alluvial fan to significantly fluctuate; therefore, the grid with sudden ground subsidence may be more variable. On the other hand, the four emergency water sources are all located in the middle and upper part of the alluvial fan. Affected by the exploitation, the groundwater level changes markedly, resulting in greater fluctuations in land subsidence. Furthermore, at the edge of the Quaternary groundwater drop funnel, the grid with mutation in the land subsidence rate is very variable. This shows that the boundary of the groundwater funnel is the place where the groundwater level changes most, and the land subsidence is relatively fragile and unstable.

4 Conclusions

The main conclusions of this study are as follows:

1. From 2004 to 2015, the maximum land subsidence rate was -141 mm yr^{-1} .
2. The single-year mutation cells were mainly distributed in the middle and lower parts of the alluvial–diluvial fans of the Yongding and Chaobai rivers. The multiple-year grid mutations were mainly distributed in the middle and upper parts of the alluvial fan, near the emergency water source and at the edge of the underground water funnel.

Data availability. No data sets were used in this article.

Author contributions. LG performed the experiments, analyzed the data and wrote the paper. HG, XL and ZZ provided crucial guidance and support throughout the research. LW and YM contributed significantly to the validation work and data interpretation.

Competing interests. The authors declare that they have no conflict of interest.

Special issue statement. This article is part of the special issue “TISOLS: the Tenth International Symposium On Land Subsidence – living with subsidence”. It is a result of the Tenth International Symposium on Land Subsidence, Delft, the Netherlands, 17–21 May 2021.

Acknowledgements. We thank both the European Space Agency (ESA) and the Canadian Space Agency for their great efforts in developing and distributing the remotely sensed SAR data. We also thank the China Geological Survey (CGS) for the leveling data released to the public. Moreover, we are grateful to the National Aeronautics and Space Administration (NASA) for making the SRTM DEM data available. Finally, we acknowledge the creators of the Python computer language and ArcGIS software as well as the Doris/SARPROZ and StaMPS/QPS data processing software.

Financial support. This work was supported by the National Natural Science Foundation of China (grant nos. 41930109/ D010702 and 41771455/ D010702) and the General Scientific Research Plan project of the Beijing Municipal Commission of Education (grant no. KM202010028011).

References

Albano, M., Polcari, M., Bignami, C., Moro, M., Saroli, M., and Stramondo, S.: An innovative procedure for monitoring the

change in soil seismic response by InSAR data: Application to the Mexico City subsidence, *Int. J. Appl. Earth Obs. Geoinf.*, 53, 146–158, <https://doi.org/10.1016/j.jag.2016.08.011>, 2016.

Amighpey, M. and Arabi, S.: Studying land subsidence in Yazd province, Iran, by integration of InSAR and levelling measurements, *Remote Sens. Appl. Soc. Environ.*, 4, 1–8, <https://doi.org/10.1016/j.rsase.2016.04.001>, 2016.

Berardino, P., Fornaro, G., Lanari, R., and Sansosti, E.: A new algorithm for surface deformation monitoring based on small baseline differential SAR interferograms, *IEEE T. Geosci. Remote*, 40, 2375–2383, <https://doi.org/10.1109/TGRS.2002.803792>, 2002.

Castellazzi, P., Arroyodomínguez, N., Martel, R., Calderhead, A. I., Normand, J. C. L., Gárfias, J., and Rivera, A.: Land subsidence in major cities of Central Mexico: Interpreting InSAR-derived land subsidence mapping with hydrogeological data, *Int. J. Appl. Earth Obs. Geoinf.*, 47, 102–111, <https://doi.org/10.1016/j.jag.2015.12.002>, 2016.

Chilingar, G. V. and Endres, B.: Environmental hazards posed by the Los Angeles Basin urban oilfields: an historical perspective of lessons learned, *Environ. Geol.*, 47, 302–317, <https://doi.org/10.1007/s00254-004-1159-0>, 2005.

Da Lio, C. and Tosi, L.: Land subsidence in the Friuli Venezia Giulia coastal plain, Italy: 1992–2010 results from SAR-based interferometry, *Sci. Total Environ.*, 633, 752–764, <https://doi.org/10.1016/j.scitotenv.2018.03.244>, 2018.

Dehghani, M., Zojj, M. J. V., Hooper, A., Hanssen, R. F., Entezam, I., and Saatchi, S.: Hybrid conventional and Persistent Scatterer SAR interferometry for land subsidence monitoring in the Tehran Basin, Iran, *ISPRS J. Photogramm.*, 79, 157–170, <https://doi.org/10.1016/j.isprsjprs.2013.02.012>, 2013.

Ferretti, A., Prati, C., and Rocca, F.: Nonlinear subsidence rate estimation using permanent scatterers in differential SAR interferometry, *IEEE T. Geosci. Remote*, 38, 2202–2212, <https://doi.org/10.1109/36.868878>, 2000.

Gao, M., Gong, H., Chen, B., Li, X., Zhou, C., Min, S., Yuan, S., Zheng, C., and Duan, G.: Regional Land Subsidence Analysis in Eastern Beijing Plain by InSAR Time Series and Wavelet Transforms, *Remote Sens.*, 10, 365, <https://doi.org/10.3390/rs10030365>, 2018.

Ge, L., Ng, H. M., Li, X., Abidin, H. Z., and Gumilar, I.: Land subsidence characteristics of Bandung Basin as revealed by ENVISAT ASAR and ALOS PALSAR interferometry, *Remote Sens. Environ.*, 154, 46–60, <https://doi.org/10.1016/j.rse.2014.08.004>, 2014.

Gong, H., Yun, P., Zheng, L., Li, X., Lin, Z., Chong, Z., Huang, Z., Li, Z., Wang, H., and Zhou, C.: Long-term groundwater storage changes and land subsidence development in the North China Plain (1971–2015), *Hydrogeol. J.*, 26, 1417–1427, <https://doi.org/10.1007/s10040-018-1768-4>, 2018.

Guo, L., Gong, H. L., and Zhu, F.: Analysis of the Spatiotemporal Variation in Land Subsidence on the Beijing Plain, China, *Remote Sens.*, 11, 1170, <https://doi.org/10.3390/rs11101170>, 2019.

Lanari, R., Mora, O., Manunta, M., Mallorquí, J. J., Berardino, P., and Sansosti, E.: A small-baseline approach for investigating deformations on full-resolution differential SAR interferograms, *IEEE T. Geosci. Remote Sens.*, 42, 2375–2383, <https://doi.org/10.1109/TGRS.2004.828196>, 2004.

- Solari, L., Del Soldato, M., Bianchini, S., Ciampalini, A., Ezquerro, P., Montalti, R., Raspini, F., and Moretti, S.: From ERS 1/2 to Sentinel-1: Subsidence monitoring in Italy in the last two decades, *Front. Earth Sci.*, 6, 149, <https://doi.org/10.3389/feart.2018.00149>, 2018.
- Xue, Y. Q., Yun, Z., Ye, S. J., Wu, J. C., and Li, Q. F.: Land subsidence in China, *Environ. Geol.*, 48, 713–720, <https://doi.org/10.1007/s00254-005-0010-6>, 2005.
- Ye, S., Xue, Y., Wu, J., Yan, X., and Yu, J.: Progression and mitigation of land subsidence in China, *Hydrogeol. J.*, 24, 1–9, <https://doi.org/10.1007/s10040-015-1356-9>, 2015.
- Yin, J., Yu, D., and Wilby, R.: Modelling the impact of land subsidence on urban pluvial flooding: A case study of downtown Shanghai, China, *Sci. Total Environ.*, 544, 744–753, <https://doi.org/10.1016/j.scitotenv.2015.11.159>, 2016.
- Zhang, Y., Wu, H. A., Kang, Y., and Zhu, C.: Ground Subsidence in the Beijing-Tianjin-Hebei Region from 1992 to 2014 Revealed by Multiple SAR Stacks, *Remote Sens.*, 8, 675, <https://doi.org/10.3390/rs8080675>, 2016.
- Zhou, C., Gong, H., Chen, B., Li, J., Gao, M., Zhu, F., Chen, W., and Liang, Y.: InSAR time-series analysis of land subsidence under different land use types in the Eastern Beijing Plain, China, *Remote Sens.*, 9, 380, <https://doi.org/10.3390/rs9040380>, 2017.
- Zhu, L., Gong, H., Li, X., Rong, W., Chen, B., Dai, Z., and Teatini, P.: Land subsidence due to groundwater withdrawal in the northern Beijing plain, China, *Eng. Geol.*, 193, 243–255, <https://doi.org/10.1016/j.enggeo.2015.04.020>, 2015.